RSC Advances

ROYAL SOCIETY OF CHEMISTRY

www.rsc.org/advances

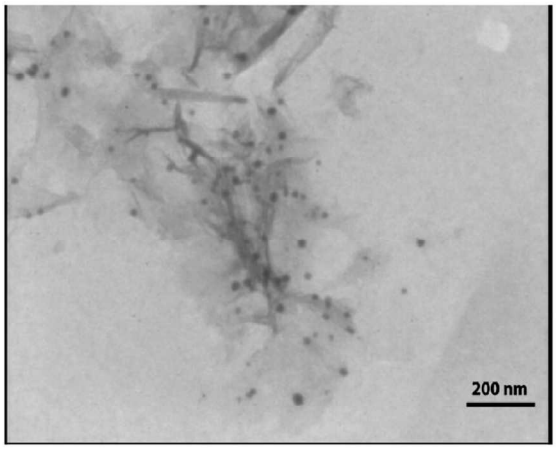

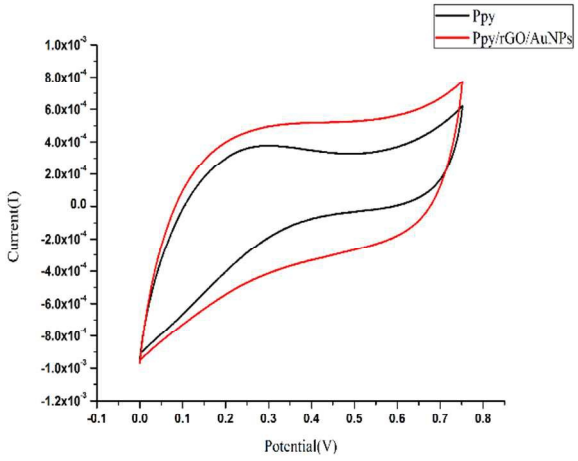

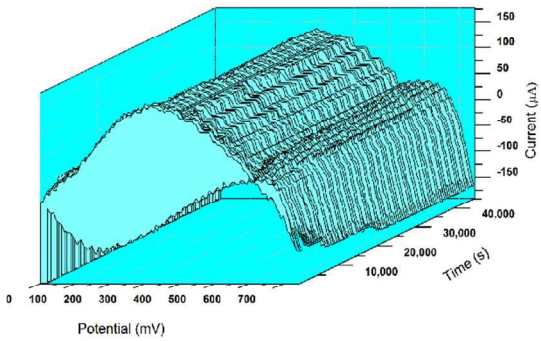

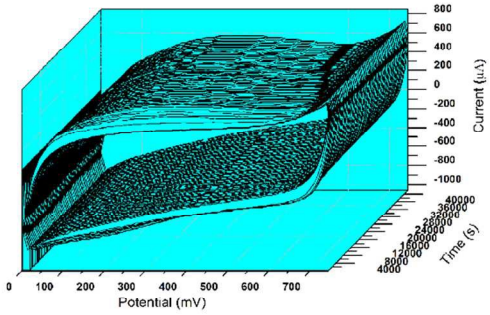

Electrochemical study of supercapacitor performance of poly pyrrole ternary nanocomposite electrode by fast fourier transform continues cyclic voltammetry

Nahideh Salehifar[1], Javad Shabani Shayeh*[2], Seyed Omid Ranaei Siadat[2], Kaveh Niknam[2], Ali Ehsani[3], Siavash Kazemi Movahhed[2]

[1-] *Department of Electric and Computer, Islamic Azad University, Science and Research Branch, Tehran, Iran*

[2-] *Protein Research center, University of Shahid Beheshti, Tehran, Iran.*

[3-] *Department of Chemistry, Faculty of science, University of Qom, P. O. Box 37185-359, Qom, Iran.*

* *Corresponding author E-mail: shabanijavad@ut.ac.ir, shabanijavad75@gmail.com*

Abstract

Supercapacitive behavior of Polypyrrole/reduced Geraphene Oxide/Au Nano particles (Ppy/rGO/AuNPs) as a ternary composite electrode was studied by cyclic voltammetry (CV), Galvanostatic charge/discharge (CD), impedance spectroscopy (EIS) and finally fast Fourier transform continues cyclic voltammetry (FFTCCV) techniques. Composite electrode was synthesized electrochemically in a 1M KCl solution containing the pyrrole monomer (0.1 M), rGO/AuNPs (0.2% wt) and 5 mM sodium dodecyl sulfate (SDS). Based CV study, Specific capacitance of Ppy and Ppy/rGO/AuNPs electrodes calculated 190 and 310 F/g respectively. CD studies showed that using rGO/AuNPs in the structure of composite electrode results to decreasing the equivalent series resistance of composite film. FFTCCV is one the novel and modern electrochemical techniques that presents useful data for study the performance of active material. The results showed that after 1200 cycles Ppy/rGO/AuNPs electrode can save its capacitance compare with Ppy electrode.

Keywords: Supercapacitor, Polypyrrole, Graphene, Au Nano particles, fast Fourier transform.

1 Introduction

Supercapacitors are one of the energy storage systems that today's have attracted the researchers attention to itself. Due to long cycle ability and high energy density, supercapacitors are under focus against dielectric capacitors and batteries[1-4]. Two categories are designed for classification of supercapacitors about the charge storage mechanism, Electrical double layer Capacitors (EDLCs) and Psudocapacitors. The first uses carbon compound as active material [5-7] and redox material act as active material in latter[8-10]. Conductive polymers (CPs) are one of the active materials that used in pseudocapacitors due to some suitable electrical properties like as high conductivity and some chemical properties such as easy synthetic procedure, good thermal and chemical stability, low cost and environmental friendliness[11, 12]. Polyaniline (PANI), polypyrrol (Ppy), polythiophene and its derivatives are most useful CPs that applied for supercapacitors[13-15]. Among of CPs, Ppy has some benefits than others such as the media that used for charge storage process, long stability than others and wider potential window[16]. nonetheless CPs have some defects, low specific capacitance and low time life are their negative points that the latter happens due to mechanical collision of counter ions with polymer filaments during charge/ discharge process [17-21]. For overcome to this points researchers suggest to combine CPs with nano materials. The process of this phenomena is that nano materials can connect CP filaments together and increase the mechanical stability of composite electrodes. Furthermore using nano materials in polymer matrix can enhanced the capacitance of polymer electrode[2, 13, 17, 22-25]. Carbonaceous and metal compounds are materials that combined by CPs. Carbon materials by increasing the surface of composite electrode and metal compound with a redox reaction join in charge storage mechanism and enhance the capacitance of supercapacitors[26-29].

Graphene is a carbon material that created a new aspect in electrochemistry. Good electrical conductivity, high surface area and capability of this material to get composite with CPs are some of graphene features[16, 30-36]. By using some high conductive metals like as Au nanoparticles in the structure of graphene sheets one can promote the electron transfer properties of graphene that can increase the capacitance of this material and therefore CPs-graphene composites [33, 35, 37]. In previous work we reported the super capacitive behavior of PANI/ nano structural manganese oxides using fast Fourier transform consecutive cyclic voltammetry (FFTCCV)[11]. The results showed that this electrochemical method was very suitable technique for study the performance of composite materials. In this work we presented the supercapacitive study of Polypyrrol/reduced Graphene Oxide/ Au nanoparticles (Ppy/rGO/AuNPs) in acidic media using FFTCCV technique. We synthesized composite by electrochemical method and after characterization study the electrochemical performance of this composite electrode in 0.1M H_2SO_4 solution performed.

2 Experimental

All the chemical materials used in this work were Merck products with analytical grade and were used without further purification. Double distilled water was used throughout all experiments.

2.1 Materials characterization and electrochemical evaluation

Electrochemical experiments were carried out by an Auto lab General purpose System PGSTAT 30 (Eco-chime, Netherlands). A conventional three electrode cell with a glassy carbon electrode with the area of 0.03 cm^2 as working electrode, Platinum wire and an Ag/AgCl reference electrode (Argental, 3 M KCl) were used as counter and reference electrode, respectively. The EIS experiments were conducted in the frequency range between 100 kHz and 15 mHz with perturbation amplitude of 5 mV. Morphological investigations of the polymeric films were carried out by using SEM (Philips XL 30). X-ray diffraction patterns were obtained from an X-ray diffractometer (PANalytical X'Pert-Pro) with a Cu-K^{α} monochromatized radiation source and a Ni filter.

2.2 FFTCCV technique

The FFT experimental data collection was performed with the help of the following equipment; a setup of a computer, equipped with a data-acquisition board (PCL-818HG, Advantech. Co.) And a custom-made potentiostat described in our previous works[3, 4, 11]. A computer program that was developed in Delphi6® environment used for data acquisition and data processing. The signal Calculation in this method established based on the integration of net current changes over the scanned potential range. It must be noted that in this case, the current changes at the voltammograms can be caused by various

processes, which take place at the electrode surface or matrix of CP and composite film. In detail, a CV of the electrode was firstly recorded. Then, the existing high frequency noises were indicated by applying FFT on the collected data. With the help of this information, the cutoff frequency of the analog filter was set at a certain value where the noises were removed from the CV.

2.3 Preparation of graphene oxide (GO) and rGO/Au NP

rGO/ AuNPs was synthesized as described in our previous report [37]. Graphite (10 g) and concentrated H_2SO_4 (230 mL) were stirred at constant temperature. In this method the temperature must keep below 20 °C. Simultaneously $KMnO_4$ was added to suspension such that the temperature of the mixture was fixed during the addition. After that the reaction temperature was changed to 40 °C and the mixture was stirred for 1h. Then 500 ml deionized water was added to the reaction cell by increasing the temperature to 100 °C. After this step H2O2 (2.5 ml) was added slowly, followed by addition of deionized water (500 mL). Then, the solution was washed with HCl (200 mL) and deionized water until the filtrate became neutral and the remaining impurities were removed. The product, graphite oxide, was exfoliated in deionized water in an ultrasonic bath to form graphene oxide (GO) nanosheets.

The GO powder was added to water dispersed Au nanoparticles and uniformly dispersed by sonication for 1 h. This suspension was then stirred 24 h at 40 °C. Afterwards, the mixture was filtered using a Buchner funnel and washed with deionized water three times. The final product was dried at 50 °C for 12 h. The XRD pattern and EDS spectrum of rGO /AuNPs is shown in Fig. 1. The diffraction peaks at 38.1°, 64.5° and 77.5° correspond to (111), (220) and (311) planes of AuNPs, respectively. Moreover, an additional peak is observed at about of 43.6°, which seems to be due to overlapping (200) reflection plane of Au, at $2\theta = 44.4°$, with (100) plane of graphite[38, 39]. Furthermore, Table 1 shows

the results that measured by EDX analysis of rGO/AuNPs. As can be seen the weight percentage of AuNPs is low.

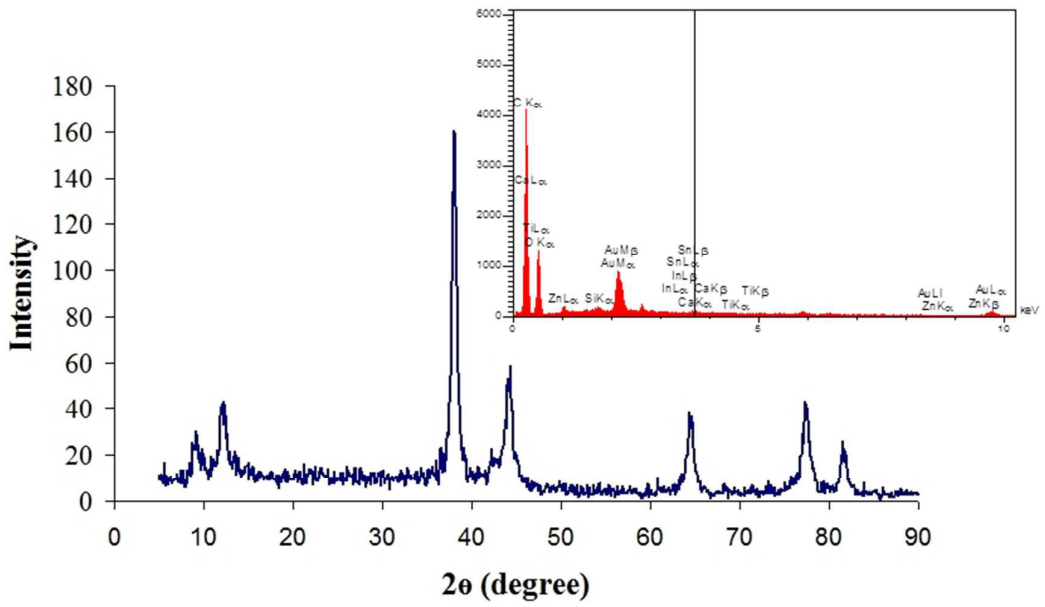

Fig. 1. XRD pattern and EDX spectrum of rGO/AuNPs

Table 1. Results for EDX analysis of rGO/AuNPs.

Element	Line	W%	A%
C	Ka	61.92	68.72
O	Ka	37.5	31.24
Au	La	0.58	0.04
		100	100

2.4 Synthesis of Ppy and Ppy/rGO/AuNPs composite electrodes

Ppy/rGO/AuNPs composite was synthesized by CV technique in 1M KCl solution contained pyrrol monomer (0.1M), rGO/AuNPs (0.2% wt) and sodium dodecyl sulfate (0.005 M) that dispersed in solution by sonication. Ppy electrode was synthesized in same solution without rGO/AuNPs and sodium dodecyl sulfate. Electro polymerizations were conducted by 10 cycles at the sweep rate of 50 mV/s in the potential of 0 to 1 V. The mass of Ppy films was approximated assuming a current efficiency for the electropolymerization process of 100%, using $Q = \frac{n_e F m_{Ppy}}{M_{Ppy}}$ equation . Where n_e = 2.30 accounts for 2.30 electrons per pyrrole during electrodeposition to form the partially oxidized Ppy (0.30 e more than the required 2e for forming native Ppy) [40, 41].

Fig. 2. Illustrate TEM, SEM graphs of rGO/AuNPs, Ppy and Ppy/rGO/AuNPs composite film. As evident the rGO sheets exhibit rippled and crumpled morphology and have a structure consisting of very thin layers. From Fig. 2(c, d) one can determine distinguishable differences between Ppy and Ppy/rGO/AuNPs film. As illustrate, rGO/AuNPs distributed in Ppy network to form composite film and Au nanoparticles that presented in TEM graph are very small in size.

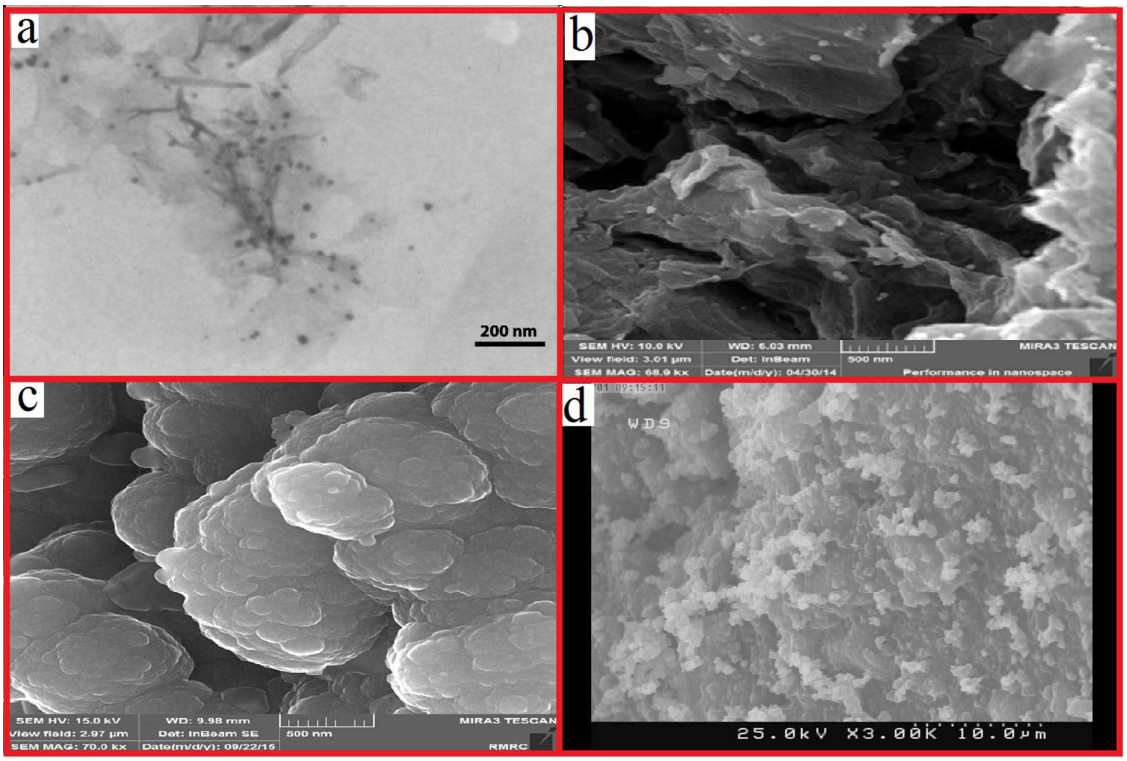

Fig. 2. TEM graph of rGO/AuNPs (a) SEM images of rGO/AuNPs (b) Ppy (c) and Ppy/rGO/AuNPs electrodes (d).

3 Results and discussion

CV is one the electrochemical techniques which provide very useful information about the nature of various electrode in different media[21, 42, 43]. Fig. 3 presents the CVs of Ppy and Ppy/rGO/AuNPs electrodes in 0.1M H_2SO_4 solution at the scan rate of 25mV/s. As can be seen the shape of CVs for two electrode are different together in that the area that surrounded by CV curve for ternary composite electrode is much more than Ppy electrode. The SC of two electrodes can be calculate by use the following equation:

$$C = \frac{I}{mv} \qquad (1)$$

Where I is the current, m is the mass of reactive material and ν is the potential scan rate. The SC of Ppy and Ppy/rGO/AuNPs electrodes were found to be 190 and 310 F/g, respectively. There are two type of contribution in the composite structure that leads to enhancement in capacitive behaviors of electrode. Electric double-layer capacitance produced by graphene and pseudo capacitive behavior of Ppy that attributed to the structure of the ternary film electrodes. In comparison with electrochemical performance of individual material, using rGO/AUNPs with very low amount can enhance the SC of composite electrode very distinctively that shows the synergistic effect of rGO/AuNPs in Ppy network[37, 44, 45]. Furthermore, the stability of current is another feature of ternary composite electrode. As can be seen in Fig. 3 for Ppy electrode the current in anodic sweep reach to a maximum at 0.2V and then decreased. But this phenomena didn't occurs for Ppy/rGO/AuNPs and the current in CV of composite electrode save its symmetrical shape compare with Ppy one.

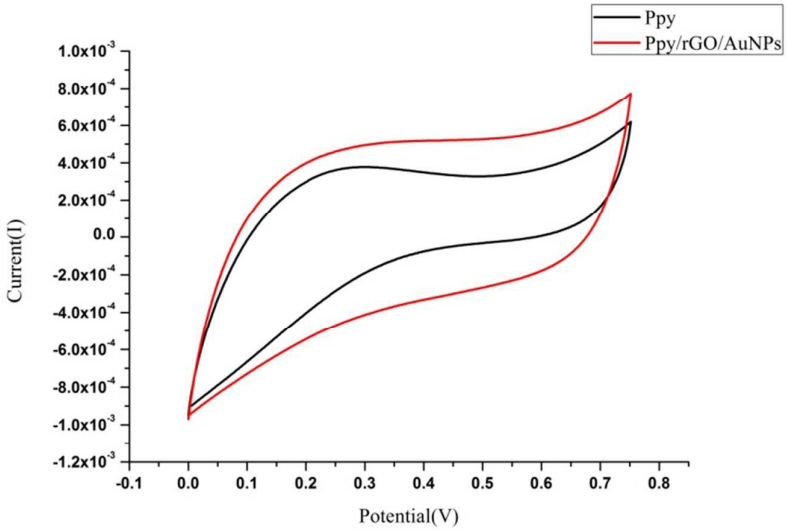

Fig. 3. CVs of Ppy and Ppy/rGO/AuNPs electrodes in 0.1M H_2SO_4 solution at the scan rate of 25mV/s.

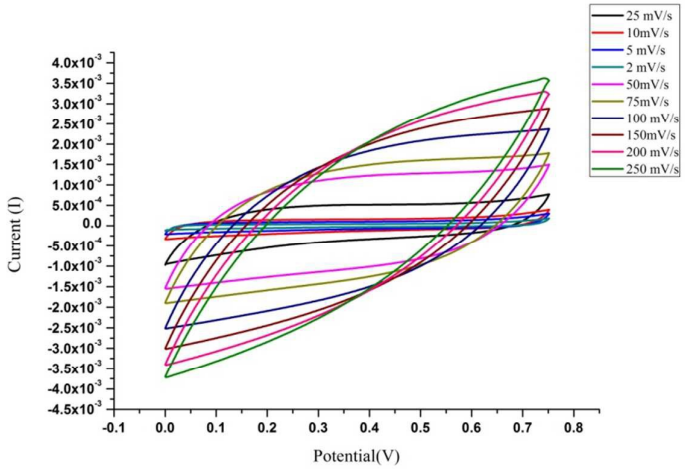

Fig. 4. CVs of Ppy/rGO/AuNPs electrodes at various scan rate in 0.1M H_2SO_4 solution.

One of the electrochemical properties of supercapacitor electrodes that show their kinetic performance is the behavior at various scan rates. Fig. 4. Shows CV curves of Ppy/rGO/AuNPs electrode at various scan rates in 0.1 M H_2SO_4 media. As presented, the excellent capacitive performance of the Ppy/rGO/AuNPs electrode is verified from these curves. As can be seen, CV curves of Ppy/rGO/AuNPs save their rectangular shape by increasing scan rate. This behavior can be related to an ideal capacitive performance of

Ppy/rGO/AuNPs electrode [46]. Ppy/rGO/AuNPs electrode save its rectangular CCV shape until the scan rate of 100 mV/s. The deviation from rectangularity of CVs becomes obvious as scan rate increases. This phenomenon can be attributed to the electrolyte and film resistance, and this distortion is dependent on scan rate. By increasing the sweep rate deeper active sites in composite material will not have enough time for reaction with ions from solution.

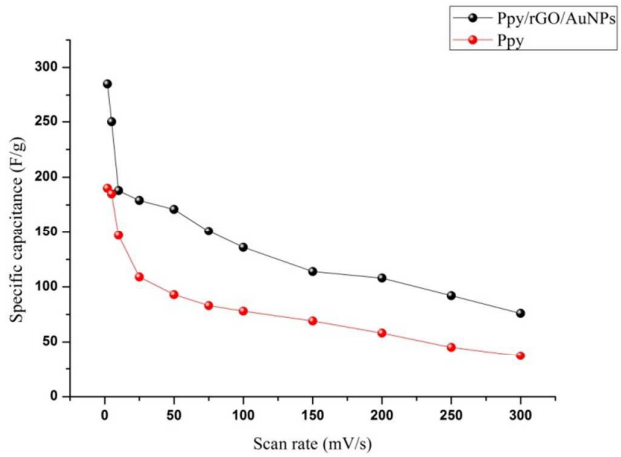

Fig. 5. Specific capacitance of Ppy and Ppy/rGO/AuNPs composite electrodes as a function of scan rate in 0.1M H_2SO_4 solution.

Fig. 5. Presents the relation between the specific capacitance (SC) of two electrodes with scan rate in 0.1M H_2SO_4 solution. Ppy/ rGO /AuNPs composite electrode shows specific capacitances of 290 and 85 F/g at the scan rate of 2 and 300 mV/s, respectively, whereas specific capacitances of the Ppy electrode decreases from 195 to 45 F/g at the scan rate of 2 and 300 mV/s, respectively. As observed, the capacitance of two electrodes decreased over the entire range of scan rate, because in fast sweep rates just outer porosities are use and deeper those are not accessible for dope/ undope process[11]. In Fig. 5. There are two slope for decreasing the capacitance for two electrodes. This phenomena create this idea that there are two type of active sites in both matrix electrodes. One of the important parameters that can describe the type of active site is the slope of change in SC vs. scan rate diagram. As can be seen from Fig. 5 the SC for

ternary electrode change by a lower slope than Ppy one which shows the accessible active sites for composite electrode are more than Ppy film due to independency of SC to scan rate.

To highlight the capacitance characteristic of Ppy/rGO/AuNPs ternary composite electrode Galvanostatic charge/discharge technique has been used. Fig. 6. shows the charge/discharge behavior of Ppy and Ppy/rGO/AuNPs electrodes in the potential range from 0 to 0.75 V at the current density of 0.9 A/g. the triangular shape between this potential range indicate good columbic efficiency and ideal capacitive behavior of Ppy/rGO/AuNPs as an electrode for supercapacitors. Furthermore, using rGO /AuNPs caused to decrease the equivalent series resistance (ESR) for Ppy/rGO/AuNPs composite electrode. This is related to the internal resistance and appears in the curves during the change of current sign and vice versa.

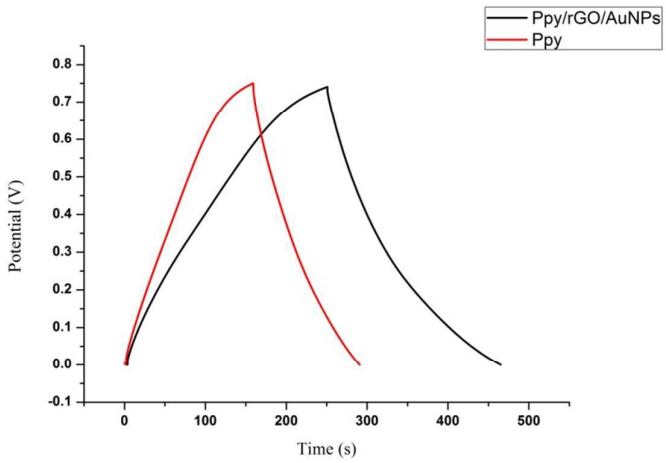

Fig. 6. Galvanostatic charge and discharge measurements of Ppy and Ppy/ rGO /AuNPs electrode in 0.1M H_2SO_4 solution at the current density of 0.9A/g.

The specific capacitance of two electrodes from Fig. 6 can be calculated by following equation:

$$SC = \frac{i}{\left(-\frac{\Delta E}{\Delta t}\right)m} \qquad (2)$$

In this equation $\frac{\Delta E}{\Delta t}$ is the slope of the discharge curve after the voltage drop at the beginning of each discharge (ESR); and m was the mass of composite electrodes. The calculated SC were 120 and 190 F/g for Ppy and Ppy/rGO/AuNPs electrodes respectively.

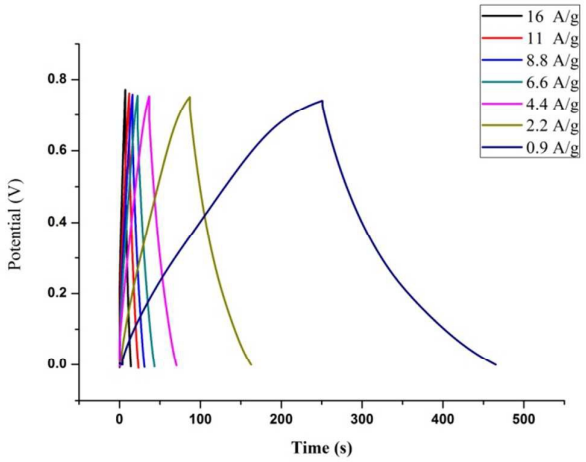

Fig. 7. Galvanostatic Charge-Discharge curves of Ppy/ rGO /AuNPs electrode at 0.9, 2.2, 4.4, 6.6, 8.8, 11 and 16 A/g in 0.1 M H_2SO_4 solution.

Fig. 7. Presents the charge−discharge curves of Ppy/rGO/AuNPs electrode at various specific currents. As can be seen the SC magnitudes of ternary composite electrode decreased by enhancing the specific current that is due to intercalation of ions at the surface of the active materials in the electrode/electrolyte interface. Another description is that in low specific currents there is enough time for insertion and deinsertion of ions in to the all porosities of the active materials in the electrode/electrolyte interface. The most SC for composite electrode is obtained when the current density for charge/discharge process is 0.9 A/g.

For investigation some electrochemical supercapacitive and conductivity behaviors of two electrodes EIS technique is performed.

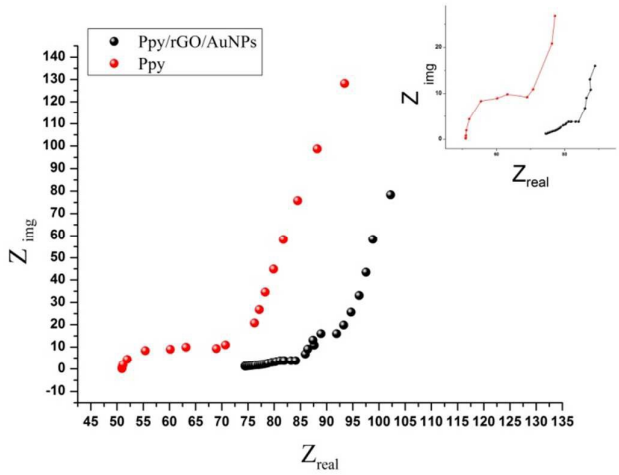

Fig. 8. Nyquist plots recorded from 10 kHz to 0.01 Hz with an ac amplitude of 5 mV for Ppy and Ppy/rGO/AuNPs electrode in 0.1M H_2SO_4 solution.

Nyquist plots of Ppy and Ppy/rGO/AuNPs electrodes at open circuit potential (OCP) illustrated in Fig. 8. As can be seen the solution resistance (R_s) can found by reading the real axis value at the high frequency intercept for both electrode. Difference between the magnitudes of R_s can be attributed to differences in ohmic resistance of two electrode or the amount of OCP that applied for electrodes. As presented in the figure both plots have a semicircle in high frequencies which is related to the charge transfer resistance caused by the Faradic reactions and the double-layer capacitance (C_{dl}) at the contact interface between electrode and electrolyte solution. A resistance with the slope of the 45° in the curve that called Warburg resistance (Z_W) is a result of the frequency dependence of ion diffusion/transport from the electrolyte to the electrode surface[31, 47-49].

As observed from Fig. 8, the magnitude of R_{ct} in Ppy/rGO/AuNPs electrode was smaller than that in Ppy film, which shows the presence of rGO/AuNPs in polymer matrix enhanced the conductivity and charge transfer performance of composite electrode. The low frequency capacitance (C_{lf}) of each film was determined from Eq. (3).

$$C_{lf} = \frac{1}{(2\pi f Z'')} \quad (3)$$

In this equation Z" is the imaginary component of impedance at lowest frequency in Nyquist diagram (*f*).

From this equation the SC of Ppy and Ppy/rGO/AuNPs electrodes were calculated 160 and 280F/g, respectively. These results showed that the SC of ternary composite electrode is near two times more than polymer one. Furthermore CV, CD results confirmed the data that obtained by EIS method.

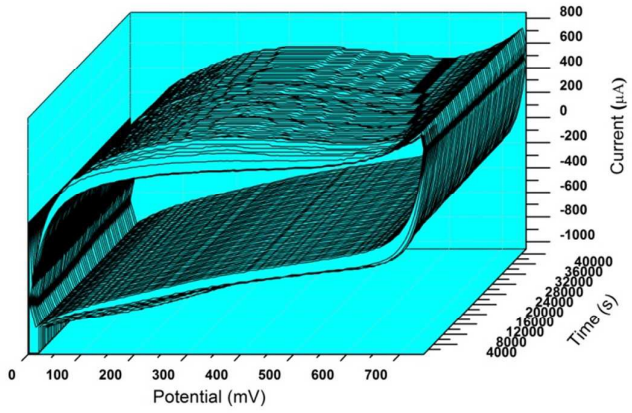

Fig. 9. 3D cyclic voltammograms of Ppy/rGO/AuNPs ternary electrode as a function of time in H_2SO_4 0.1M at the scan rate of 50mV/s.

FFTCCV technique could be considered as the best tool for examination the changes in the CVs and charge storage of a capacitor during the time. furthermore by using this technique one can study the behavior of electrochemical system momentarily[11]. The change in electrochemical behavior of composite electrode can be observed in the 3D CVs in over time. CVs of composite electrode in the range of 0-40000s presented in Fig. 9. As illustrated, in the whole range of time the composite electrode saves its symmetrical shape and just at the beginning of experiment the CVs improved and get wider. This phenomena can be attribute to this reason that in the primary CVs there are

some impurities that block some active sites of composite electrode and after sweeping, this impurities removed from the matrix of composite and therefore those active site can join to the reaction process.

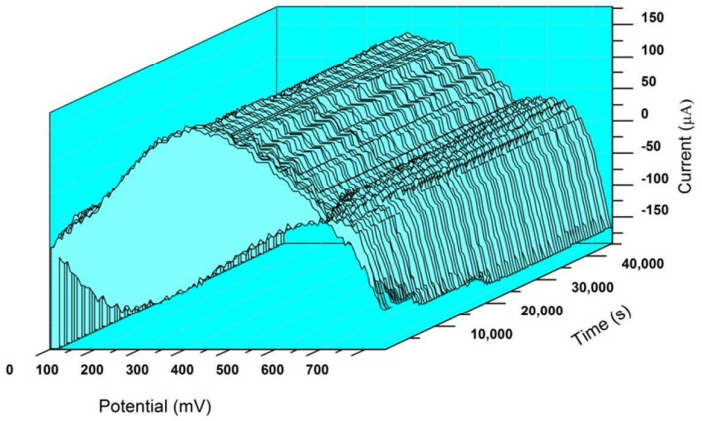

Fig. 10. 3D differential voltammograms of Ppy/rGO/AuNPs electrode measured at 50 mV s^{-1}.

Fig. 10. Presents 3D differential CVs of composite electrode that obtained from Fig. 9. Some useful information about the performance of electrode can be resulted from this figure. As can be seen by increasing the time, oxidation part of diagrams changed and the area that surrounded by diagrams get lower. Although the composite electrode can save its whole shape but after time duration, CVs of composite electrode loss their fixity inchmeal. Change in the shape of diagram related to drop of current in the oxidative half cycles of composite electrode[11].

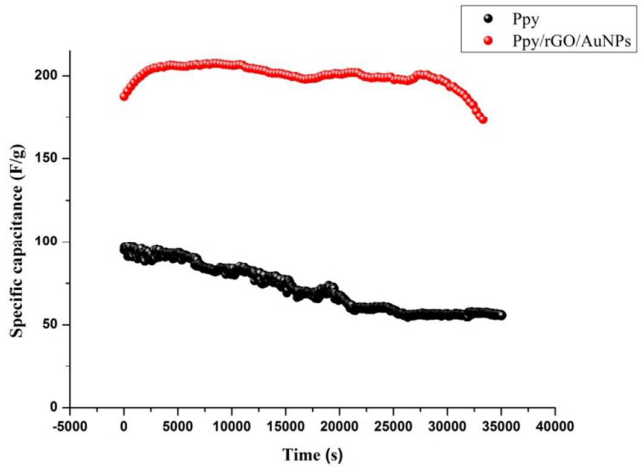

Fig. 11. Stability of two electrode as a function of time in H_2SO_4 0.1M at the scan rate of 50mV/s.

Another feature of CPs for using as active material in supercapacitors is the stability of these electrodes after continues cycles. Fig. 11 presents the stability of two electrodes using consecutive CVs in H_2SO_4 0.1M at the scan rate of 50mV/s. As can be seen Ppy electrode in the time range between 0-35000 s lose its capacitance near 50% but this phenomena doesn't occurs for ternary composite electrode. As showed, Ppy/rGO/AuNPs electrode save its capacitance in this time range. The pattern shows, at the initial cycles the SC of composite electrode increased from 180 to 204 F/g that can be attributed to this fact that in firstly cycles there are some active site and porosities in the composite electrode that occupied by some impurities and maybe solvent molecules. By conducting the cycles these materials exited from those sites and therefore the number of active sites of composite electrode enhanced. This modification of composite film results to increase the SC of composite film. After growth, the SC of Ppy/rGO/AuNPs electrode be constant until 30000 s and then decreased. The sharp decrease in the stability percentage of composite electrode can be attribute to block some of active sites with negative ions or degradation of polymer chains due to change in polymer volume in dope/undope process. This results showed that using rGO/AuNPs into Ppy

matrix can evaluated the stability of composite electrode through consecutive cycles.

4 Conclusion

In this paper some electrochemical features of Ppy/rGO/AuNPs as a ternary composite electrode for using in supercapacitors were studied. The data showed that using rGO/AuNPs in the structure of Ppy electrode results to increasing the capacitance of composite electrode, decrease the ESR of composite electrode and enhance the stability of composite film through consecutive CVs. FFTCCV is one of the applicable and useful technique for study the performance of supercapacitive material. Study the electrochemical performance and stability of electrodes are the advantage of using this technique.

Acknowledgements

The authors are grateful to the Research Council of University of Shahid Beheshti and Iranian Nano Council for the financial support of this work.

5 References

1. P. Simon and Y. Gogotsi, *Nature materials*, 2008, **7**, 845-854.
2. X. Zhang, X. Zeng, M. Yang and Y. Qi, *ACS applied materials & interfaces*, 2014, **6**, 1125-1130.
3. J. S. Shayeh, P. Norouzi, M. R. Ganjali, M. Wojdyla, K. Fic and E. Frackowiak, *RSC Advances*, 2015, **5**, 84076-84083.
4. J. S. Shayeh, A. Ehsani, A. Nikkar, P. Norouzi, M. R. Ganjali and M. Wojdyla, *New Journal of Chemistry*, 2015, DOI: 10.1039/C5NJ01954K.
5. G. J. Wilson, M. G. Looney and A. Pandolfo, *Synthetic Metals*, 2010, **160**, 655-663.
6. B. E. Conway, 1999.
7. M. Endo, T. Takeda, Y. Kim, K. Koshiba and K. Ishii, *Carbon science*, 2001, **1**, 117-128.
8. C. Arbizzani, M. Mastragostino and B. Scrosati, *Organic Conductive Molecules and polymers, cap*, 1997, **5**, 595.
9. C. Arbizzani, M. Mastragostino and F. Soavi, *Journal of power sources*, 2001, **100**, 164-170.
10. M. A. Bavio, G. G. Acosta and T. Kessler, *Journal of Power Sources*, 2014, **245**, 475-481.
11. J. Shabani Shayeh, P. Norouzi and M. R. Ganjali, *RSC Advances*, 2015, **5**, 20446-20452.
12. A. H. Gemeay, I. A. Mansour, R. G. El-Sharkawy and A. B. Zaki, *European polymer journal*, 2005, **41**, 2575-2583.
13. L. L. Zhang, S. Li, J. Zhang, P. Guo, J. Zheng and X. Zhao, *Chemistry of Materials*, 2009, **22**, 1195-1202.
14. C. Li, H. Bai and G. Shi, *Chemical Society Reviews*, 2009, **38**, 2397-2409.
15. X. Xia, W. Lei, Q. Hao, W. Wang and X. Wang, *Electrochimica Acta*, 2013, **99**, 253-261.
16. S. Biswas and L. T. Drzal, *Chemistry of Materials*, 2010, **22**, 5667-5671.
17. Y. Yan, Q. Cheng, G. Wang and C. Li, *Journal of Power Sources*, 2011, **196**, 7835-7840.
18. A. Ahmad, P. Mukherjee, S. Senapati, D. Mandal, M. I. Khan, R. Kumar and M. Sastry, *Journal*, 2003, **28**, 313-318.
19. A. Ehsani, M. Mahjani, M. Bordbar and R. Moshrefi, *Synthetic Metals*, 2013, **165**, 51-55.
20. A. Ehsani, M. Mahjani and M. Jafarian, *Synthetic Metals*, 2011, **161**, 1760-1765.
21. A. Ehsani, M. Mahjani and M. Jafarian, *Synthetic Metals*, 2012, **162**, 199-204.

22. Z. H. Zhou, N. C. Cai, Y. Zeng and Y. H. Zhou, *Chinese Journal of Chemistry*, 2006, **24**, 13-16.
23. X. Zhang, L. Ji, S. Zhang and W. Yang, *Journal of Power Sources*, 2007, **173**, 1017-1023.
24. M. Wu, G. A. Snook, V. Gupta, M. Shaffer, D. J. Fray and G. Z. Chen, *Journal of Materials Chemistry*, 2005, **15**, 2297-2303.
25. J. Wang, Y. Xu, X. Chen and X. Sun, *Composites Science and Technology*, 2007, **67**, 2981-2985.
26. M. Toupin, T. Brousse and D. Bélanger, *Chemistry of Materials*, 2004, **16**, 3184-3190.
27. P. Taberna, P. Simon and J.-F. Fauvarque, *Journal of The Electrochemical Society*, 2003, **150**, A292-A300.
28. A. B. Stepanov, I. N. Varakin and V. V. Menukhov, *Journal*, 1999.
29. L. Shao, J.-W. Jeon and J. L. Lutkenhaus, *Chemistry of Materials*, 2011, **24**, 181-189.
30. X. Dong, W. Huang and P. Chen, *Nanoscale Res Lett*, 2011, **6**, 60.
31. Z. Fan, J. Yan, T. Wei, L. Zhi, G. Ning, T. Li and F. Wei, *Advanced Functional Materials*, 2011, **21**, 2366-2375.
32. H. Wang, Q. Hao, X. Yang, L. Lu and X. Wang, *ACS applied materials & interfaces*, 2010, **2**, 821-828.
33. Q. Xu, S.-X. Gu, L. Jin, Y.-e. Zhou, Z. Yang, W. Wang and X. Hu, *Sensors and Actuators B: Chemical*, 2014, **190**, 562-569.
34. H. Yang, W. Zhou, B. Yu, Y. Wang, C. Cong and T. Yu, *Journal of Nanotechnology*, 2012, **2012**.
35. H. Yu, P. Xu, D.-W. Lee and X. Li, *Journal of Materials Chemistry A*, 2013, **1**, 4444-4450.
36. A. Ehsani, M. G. Mahjani, M. Bordbar and S. Adeli, *Journal of Electroanalytical Chemistry*, 2013, **710**, 29-35.
37. J. S. Shayeh, A. Ehsani, M. Ganjali, P. Norouzi and B. Jaleh, *Applied Surface Science*, 2015, **353**, 594-599.
38. C. Wolf and H. Xu, *Chemical Communications*, 2011, **47**, 3339-3350.
39. J. Zhang, J. Ma, J. Jiang and X. Zhao, *Journal of Materials Research*, 2010, **25**, 1476-1484.
40. Y. Fang, J. Liu, D. J. Yu, J. P. Wicksted, K. Kalkan, C. O. Topal, B. N. Flanders, J. Wu and J. Li, *Journal of Power Sources*, 2010, **195**, 674-679.
41. S. Sadki, P. Schottland, N. Brodie and G. Sabouraud, *Chemical Society Reviews*, 2000, **29**, 283-293.
42. J. Shabani-Shayeh, A. Ehsani and M. Jafarian, *Journal of the Korean Electrochemical Society*, 2014, **17**, 179-186.
43. A. Ehsani, M. G. Mahjani, M. Jafarian and A. Naeemy, *Progress in Organic Coatings*, 2010, **69**, 510-516.

44. B. Andres, S. Forsberg, A. Paola Vilches, R. Zhang, H. Andersson, M. Hummelgård, J. Bäckström and H. Olin, *Nordic Pulp & Paper Research Journal*, 2012, **27**, 481-485.
45. M. Kim, C. Lee and J. Jang, *Advanced Functional Materials*, 2014, **24**, 2489-2499.
46. K.-W. Nam, K.-H. Kim, E.-S. Lee, W.-S. Yoon, X.-Q. Yang and K.-B. Kim, *Journal of Power Sources*, 2008, **182**, 642-652.
47. A. Ehsani, H. M. Shiri and J. Shabani, *RSC Advances*, 2015.
48. A. Ehsani, M. G. Mahjani, R. Moshrefi, H. Mostaanzadeh and J. S. Shayeh, *RSC Advances*, 2014, **4**, 20031-20037.
49. A. Ehsani, M. G. Mahjani, F. Babaei and H. Mostaanzadeh, *RSC Advances*, 2015, **5**, 30394-30404.